Effect of annealing temperature on photocatalytic activity of ZnO thin films prepared by sol–gel method

Jianguo Lv [a,b,c], Wanbing Gong [a], Kai Huang [d], Jianbo Zhu [a], Fanming Meng [b,c], Xueping Song [b,c], Zhaoqi Sun [b,c],*

[a] Department of Physics and Electronic Engineering, Hefei Normal University, Hefei 230061, China
[b] School of Physics and Material Science, Anhui University, Hefei 230039, China
[c] Anhui Key Laboratory of Information Materials and Devices, Anhui University, Hefei 230039, China
[d] Department of Mathematics and Physics, Anhui University of Architecture, Hefei 230601, China

ARTICLE INFO

ABSTRACT

Zinc oxide thin films are deposited on Si and quartz substrates using the sol–gel method. The thin films, annealed at 400, 600 and 800 °C respectively, are characterized by X-ray diffraction (XRD), scanning electron microscopy (SEM), atomic force microscopy (AFM), ultraviolet–visible spectrophotometer (UV–Vis), fluorescence spectrometer (FL) and the photocatalytic activity is tested by the decomposition of methyl orange dye under UV illumination. The results show that the mean grain size, surface-to-volume ratio, rms roughness and degradation efficiency of the thin films increases with increasing annealing temperature. In particular, ZnO thin film annealed at 800 °C exhibits the highest photocatalytic activity, degrading methyl orange by almost 88% in 180 min. Photocatalytic reaction mechanism of the ZnO thin films is discussed in detail, and the oxygen defects are proposed to be the active sites of the ZnO photocatalyst.

1. Introduction

Zinc oxide (ZnO), a direct wide band gap (3.37 eV) semiconductor, has stimulated great research interest due to its unique optical and electrical properties that are useful for nanolasers [1], piezo-electric anogenerators [2], solar cells [3], gas sensors [4,5], photocatalyst [6,7], and so on. Diverse

---

* Corresponding author at: School of Physics and Material Science, Anhui University, Hefei 230039, China. Tel.: +86 551 5107284; fax: +86 551 5107237.
E-mail address: szq@ahu.edu.cn (Z. Sun).

techniques have been used to prepare ZnO films, such as pulsed laser deposition (PLD) [8], chemical vapor deposition (CVD) [9], Molecular beam epitaxy (MBE) [10], magnetron sputtering [11,12] and sol–gel [13,14]. The sol–gel method has been receiving high attention since it enables us to develop low-cost and simple deposition procedure to obtain large area high quality ZnO films for technological applications.

As one of important semiconductor photocatalysts, nanostructure ZnO has attracted more interests because of its considerable photocatalytic efficiency and good stability [15]. Several works report the synthesis and high photocatalytic efficiencies of ZnO nanoparticles, powders and colloids [16–18]. But for water treatment applications, ZnO thin films are preferred to avoid the separation of the catalyst after the degradation process. Several works have been published in respect to photocatalytic properties of ZnO thin film prepared by different methods [14,19,20].

In this context, ZnO thin films were prepared on Si and quartz substrates by the sol–gel method and annealed at 400, 600 and 800 °C, respectively. Microstructure, surface morphology and optical properties of the thin films were explored. Photocatalytic activity of the thin films on methyl orange was studied and its possible mechanisms were discussed in detail.

2. Experimental

2.1. Preparation of ZnO thin films

Zinc acetate dehydrate ($Zn(CH_3COO)_2 \cdot 2H_2O$) and mono-ethanolamine were used as Zn source and stabilizing agent, respectively. Zinc acetate dehydrate was dissolved in a mixture of 2-methoxyethanol and mono-ethanolamine. The concentration of zinc acetate was 0.5 mol/L and the molar ratio of mono-ethanolamine to zinc acetate was kept at 1:1. The mixture solution was stirred at 60 °C for 2 h to yield a clear and homogeneous solution. After the solution was made 1 day at room temperature, it was coated on Si and quartz substrates (15 mm × 15 mm) at 3000 rpm for 30 s. Then precursor thin films were heated at 150 °C for 10 min to remove the solvent and organic residuals. The coating and heating process was repeated for 10 times. Then the as-prepared thin films were inserted to a furnace and annealed in ambient atmosphere at several temperatures from 400 to 800 °C for 60 min.

2.2. Characterization

The crystallization behavior of the ZnO thin films deposited on silicon substrate was analyzed by an X-ray diffractometer (XRD, MAC M18XHF). Surface morphology of the thin films deposited on silicon substrate was measured by a scanning electron microscopy (SEM, S-4800) and an atomic force microscopy (AFM, CSPM4000) operating in contact mode. Transmission spectra of the thin films deposited on quartz substrate were obtained by an ultraviolet–visible spectrophotometer (UV-2550, SHIMADZU). Photoluminescence (PL) spectra of the thin films deposited on quartz substrate were measured in the wavelength region of 350–600 nm at room temperature by a fluorescence spectrometer (F-4500FL) with a xenon lamp as light source excited at 325 nm.

2.3. Photocatalytic activity test

Methyl orange ($C_{14}H_{14}N_3NaO_3S$), a widely used dye, was employed as a representative dye pollutant to evaluate the photocatalytic activity of ZnO thin films. The experiment was performed in a 25 mL glass container. The ZnO thin films, deposited on quartz substrate, were immersed in 10 mL 5 ppm methyl orange solutions and were irradiated with a 36 W high pressure mercury lamp, which emits visible light of 404.7, 435.8, 546.1, and 577.0–579.0 nm, and ultraviolet light of 365 nm. The distance between the sample and the high pressure mercury lamp was 3.0 cm. The transmittance of the methyl orange solution was measured at intervals of 20 min and the total irradiation time is 180 min, and then transformed into absorbance. In our previous study [19], we found that the absorbance of methyl orange at 464 nm is directly proportional to concentration. Therefore, the absorbance of the peak at 464 nm is used to evaluate the absorption of methyl orange solution with various concentrations.
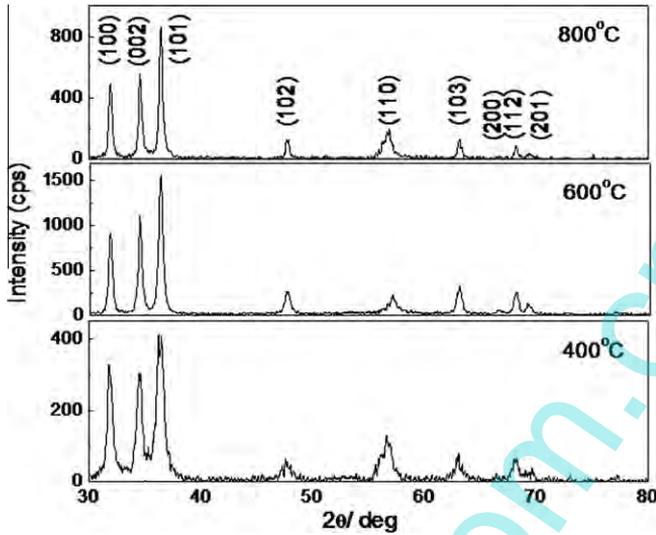
Fig. 1. XRD patterns of ZnO thin films annealed at different temperature.

The extent of photocatalytic degradation could be evaluated by measuring the absorbance of the solutions at 464 nm. The degradation efficiency of methyl orange was calculated using the equation [19]:

$$\text{Degradation}(\%) = (C_0 - C_t)/C_0 \times 100 = (A_0 - A_t)/A_0 \times 100 \tag{1}$$

where C_0 represents the initial concentration, C_t represents the concentration after t min reaction, A_0 represents the initial absorbance, and A_t represents the absorbance after t min reaction of the methyl orange at the characteristic absorption wavelength of 464 nm.

3. Results and discussion

XRD patterns of the ZnO thin film annealed at 400, 600 and 800 °C, respectively, are presented in Fig. 1. All the diffraction peaks of the ZnO thin films can be indexed to (1 0 0), (0 0 2), (1 0 1), (1 0 2), (1 1 0), (1 0 3), (2 0 0), (1 1 2) and (2 0 1) diffraction planes at $2\theta = 31.77°$, 34.42°, 36.25°, 47.54°, 56.60°, 62.86°, 66.37°, 67.96° and 69.09°,respectively (JCPDS#36-1451). The films produced are polycrystalline, showing the wurtzite ZnO hexagonal structure, while there is no evidence for the presence of other phases. The SEM and AFM images of ZnO thin films are shown in Figs. 2 and 3. It can be seen that the thin films consist of inhomogeneous and spherical-like shape nanoparticles and mean grains size of the thin films increase with increasing annealing temperature. The surface-to-volume ratio and rms roughness of the thin films obtained by AFM images are listed in Table 1. It also can be seen that the surface-to-volume ratio and rms roughness of the thin films increases with the increase of annealing temperature.

Photocatalytic tests were carried out for all the thin films. Methyl orange was used as a test contaminant. The absorption spectra of methyl orange at different irradiating intervals using ZnO thin films as photocatalyst were measured by UV–Vis spectrophotometer. Based on absorbance of methyl orange at 464 nm, degradation efficiency of methyl orange after UV irradiation for 180 min can be obtained from Eq. (1), as shown in Table 1. Curves of (C_t/C_0) versus irradiation time for the thin films annealed at different temperature are shown in Fig. 4. It can be seen that the degradation efficiency of the thin films increases with increasing annealing temperature.

According to the principles of ZnO photocatalysis [21,22], the conduction-band electrons and valence-band holes are generated on the surfaces of ZnO thin films when they are illuminated
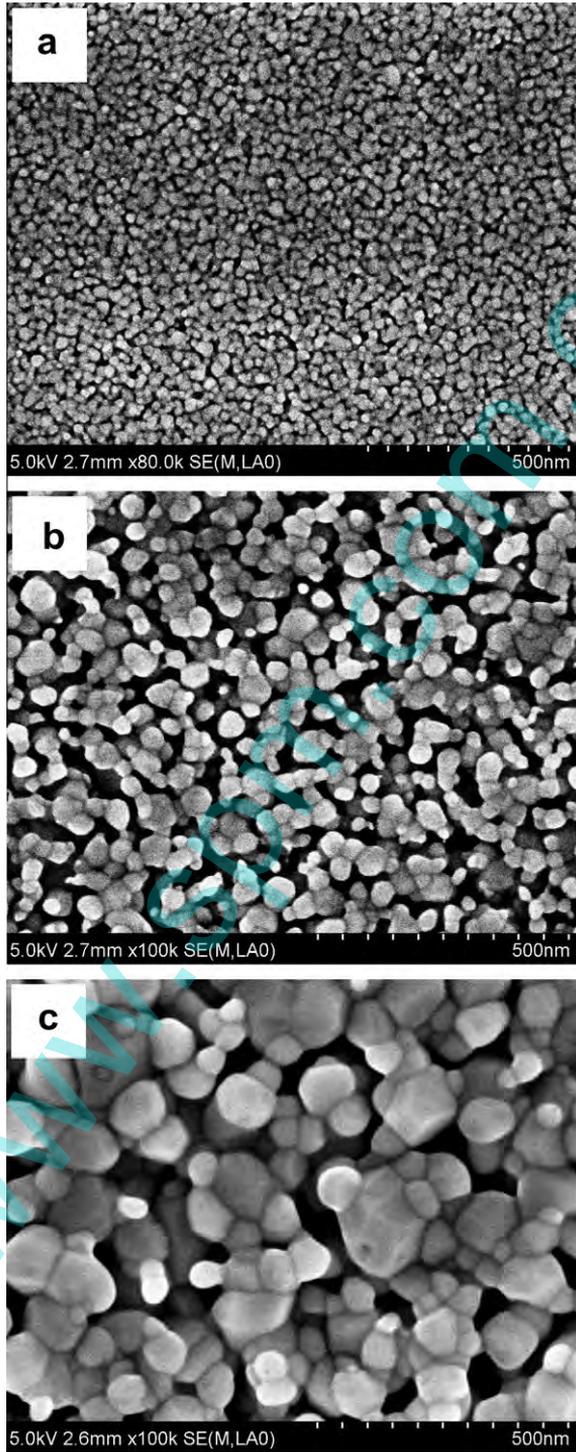
Fig. 2. SEM images of ZnO thin films annealed at (a) 400 °C, (b) 600 °C, and (c) 800 °C.
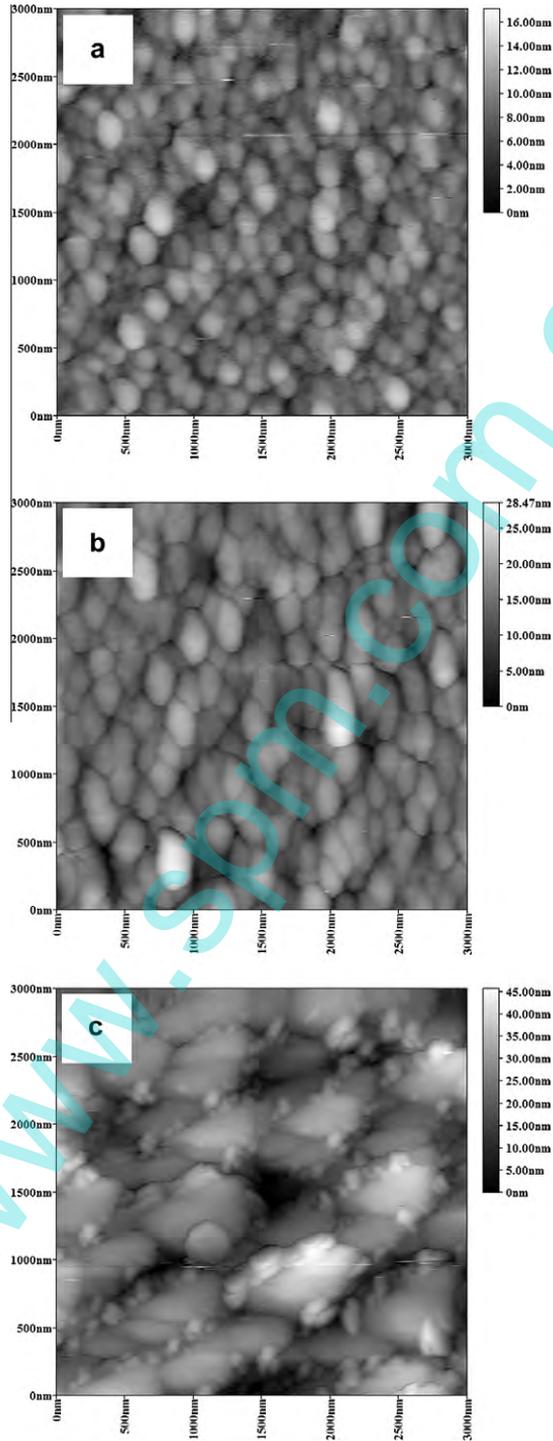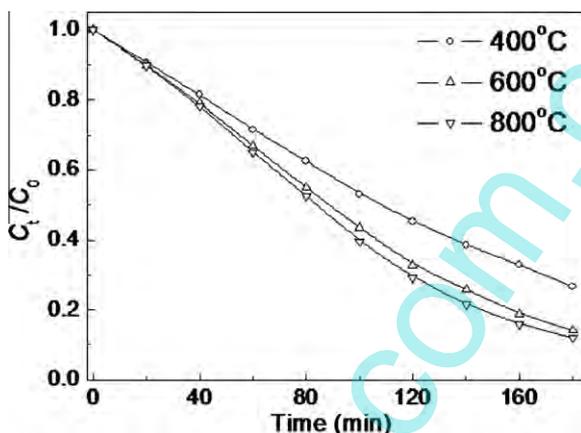
Fig. 3. AFM images of ZnO thin films annealed at (a) 400 °C, (b) 600 °C, and (c) 800 °C.

Table 1
Surface-to-volume ratio, rms roughness and degradation efficiency of ZnO thin films annealed at different temperature.

Annealing temperature (°C)	400	600	800
Surface-to-volume ratio	0.56	0.63	1.27
rms Roughness (nm)	1.95	3.37	7.44
Degradation efficiency (%)	73.4	85.8	88.0

Fig. 4. Photodegradation curves of methyl orange using ZnO thin films as photocatalysts.

by UV light with energy exceeding or equaling to its band gap energy. Holes can react with water adhering to the surfaces of ZnO thin films to form highly reactive hydroxyl radicals (OH·). Meanwhile, on the surfaces of the thin films, oxygen is reduced as an electron acceptor to superoxide and this leads to production of hydroxyl radicals (OH·). The formed radicals have a powerful oxidation ability to degrade organic dye. The reactions are summarized as below:

$$ZnO + h\nu \rightarrow e^- + h^+ \tag{2}$$

$$H_2O + h^+ \rightarrow OH^{\cdot} + H^+ \tag{3}$$

$$e^- + O_2 \rightarrow O_2^- \tag{4}$$

$$O_2^- + H^+ \rightarrow HO_2^{\cdot} \tag{5}$$

$$HO_2^{\cdot} + O_2^- + H^+ \rightarrow H_2O_2 + O_2 \tag{6}$$

$$H_2O_2 + e^- \rightarrow OH^- + OH^{\cdot} \tag{7}$$

$$OH^{\cdot} + dye \rightarrow oxidation\ products \tag{8}$$

The yield of the photo-induced electron–hole pairs depends on the intensity of incident photons with energy exceeding or equaling to the ZnO thin films band gap energy [19]. Optical transmittance spectra of the ZnO thin films in the wavelength range of 200–900 nm are depicted in Fig. 5. As shown, absorption edge for ZnO thin films shifts to longer wavelength, indicating that the band gap for ZnO thin films declines with increasing annealing temperature. Optical transmittance spectrum can be used to derive the energy gap (E_g) of the ZnO thin films [23], as shown in Fig. 6. As a result, the energy gap is 3.28, 3.27, and 3.25 eV, for the thin films annealed at 400, 600 and 800 °C, respectively.
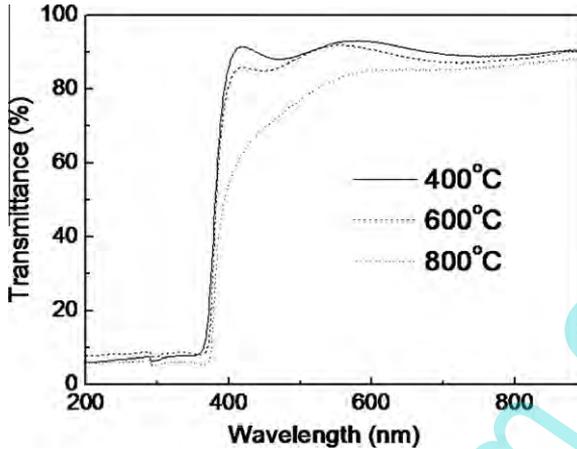
Fig. 5. Transmission spectra of ZnO thin films annealed at different temperatures.
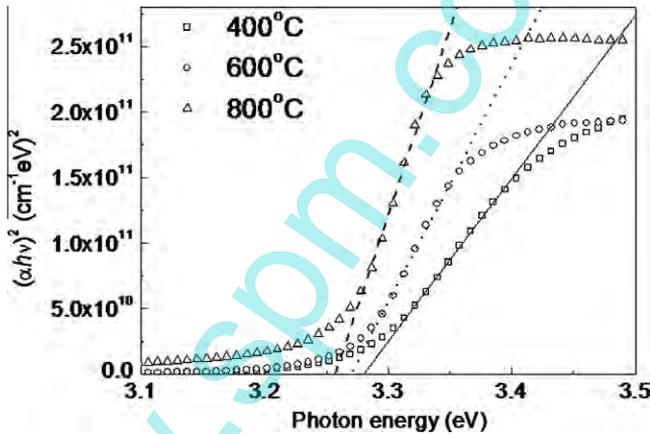

Fig. 6. $(\alpha h\nu)^2$ vs. $h\nu$ curves of the ZnO thin films annealed at different temperatures.

Accordingly, threshold absorption wavelength is 378, 380, and 382 nm, for the thin films annealed at 400, 600 and 800 °C, respectively. It can be seen that the energy gap of the ZnO thin films decreases with increasing annealing temperature, and threshold absorption wavelength increases with increasing annealing temperature. Due to our high pressure mercury lamp emits visible light of 404.7, 435.8, 546.1, and 577.0–579.0 nm, and ultraviolet light of 365 nm, we can conclude that all the thin films just absorb the ultraviolet light of 365 nm from irradiation of high pressure mercury lamp. So, the shifts of absorption edge have little effect on photocatalytic activity.

The surface-to-volume ratio, rms roughness and mean grain size are key factors influencing the photocatalytic activity. It is generally accepted that the high specific surface area and improved crystallinity degree may responsible for the increase of photocatalytic activity [24,25]. As demonstrated by SEM and AFM, the surface-to-volume ratio, rms roughness and mean grains size of the ZnO thin films increase with increasing annealing temperature. So, we can conclude that photocatalytic activity of the thin films enhances with the increase of annealing temperature.

Two impurity levels, which can enhance the electron hole pair separation rate in ZnO thin films, are generated in the presence of oxygen vacancies and interstitial oxygen defects. As the redox reactions might occur on the surface of oxygen vacancies and interstitial oxygen defects, the oxygen defects can
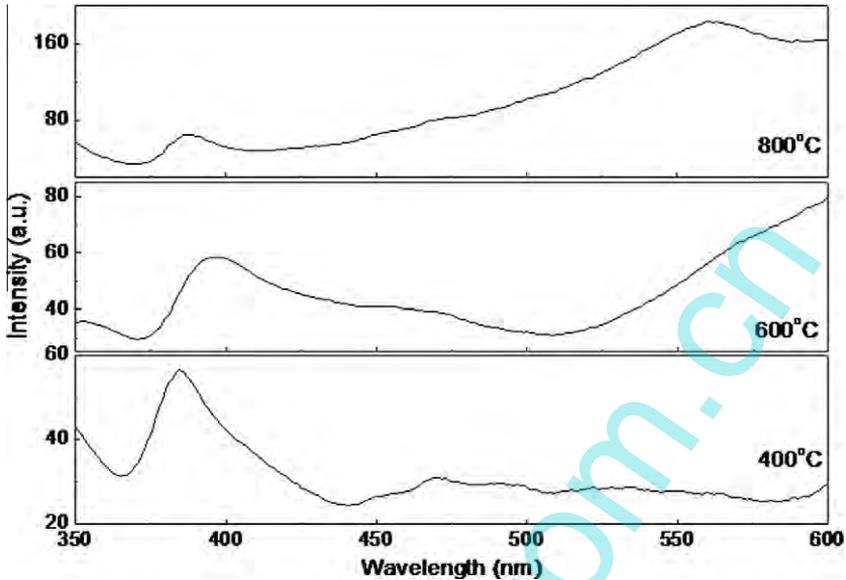
Fig. 7. PL spectra of ZnO thin films annealed at different temperatures.

be considered to be the active sites of the ZnO photocatalyst [26]. Thus, it can be suggested that oxygen vacancies and interstitial oxygen defects are in favor of photocatalytic reactions. As photoluminescence (PL) properties of ZnO are very sensitive to oxygen vacancies, we measured the PL spectra of ZnO thin films. It can be seen from Fig. 7 that the ZnO thin film annealed at 400 °C contain only a strong violet emission, the samples annealed at 600 °C and 800 °C contain a violet emission and a broad visible emission. The violet emission is called excitonic emission [27,28], which is closely related to the exciton transition from the localized level below the conduction band to the valance band. The shift of the excitonic emission may be attributed to change of the localized level below the conduction band and the carrier concentration above the valence band in the band gap [27,29]. The broad emission band revealed in the visible region is due to the superposition of green and yellow emissions. The origin of these visible emissions is still highly controversial. Generally, the green emission is typically associated with oxygen vacancy [30], and the yellow emission is associated with interstitial oxygen [31]. The two different oxygen defects are competing with each other, presenting in the competition of green and yellow bands in PL. The intensity of the visible emission of thin films increases with increasing annealing temperature, indicating that the oxygen defects of thin films increase with the increase of annealing temperature. Therefore, the photocatalytic activity of the ZnO thin films can be enhances by increasing annealing temperature.

Based on above discussion, we suggested that the increase of surface-to-volume ratio, rms roughness, and mean grain size, together with the increased oxygen defects density are main causes of enhanced photocatalytic activity for the ZnO thin films.

4. Conclusion

In summary, ZnO thin films were deposited by sol–gel method. The thin films consist of inhomogeneous and spherical-like shape nanoparticles belonging to hexagonal wurtzite structures. The absorption edge shifts to longer wavelengths with the increase of annealing temperature. The enhanced photocatalytic activity of ZnO thin films might be ascribed to the increase of surface-to-volume ratio, rms roughness, mean grain size and the oxygen defects density. The good performance of ZnO thin films

indicates that it can be used as a promising photocatalyst for the practical application in photocatalytic decolorization of organic contaminants.

Acknowledgements

References

 [1] M.H. Huang, S. Mao, H. Feick, H.Q. Yan, Y.Y. Wu, H. Kind, E. Weber, R. Russo, P.D. Yang, Science 292 (2001) 1897.
 [2] Z.L. Wang, J.H. Song, Science 312 (2006) 242.
 [3] O. Kluth, G. Schöpe, J. Hüpkes, C. Agashe, J. Müller, B. Rech, Thin Solid Films 442 (2003) 80.
 [4] N.J. Dayan, S.R. Sainkar, R.N. Karekar, R.C. Aiyer, Thin Solid Films 325 (1998) 254.
 [5] P. Mitra, A.P. Chatterjee, H.S. Maiti, J. Mater. Sci. 9 (1998) 441.
 [6] E.S. Jang, J.H. Won, S.J. Hwang, J.H. Choy, Adv. Mater. 18 (2006) 3309.
 [7] C.H. Ye, Y. Bando, G.Z. Shen, D.J. Golberg, Phys. Chem. B 110 (2006) 15146.
 [8] X.M. Fan, J.S. Lian, Z.X. Guo, H.J. Lu, Appl. Surf. Sci. 239 (2005) 176.
 [9] M.R. Waugh, G. Hyett, I.P. Parkin, Chem. Vap. Deposition 14 (2008) 366.
[10] Y.F. Chen, N.T. Tuan, Y. Segawa, H.J. Ko, S.K. Hong, T. Yao, Appl. Phys. Lett. 78 (2001) 1469.
[11] Q.P. Wang, D.H. Zhang, H.L. Ma, X.H. Zhang, X.J. Zhang, Appl. Surf. Sci. 220 (2003) 12.
[12] C.Z. Wang, P.M. Zhang, J.J. Yue, Y.Q. Zhang, L.B. Zheng, Physica B 403 (2008) 2235.
[13] B. Pal, M. Sharon, Mater. Chem. Phys. 76 (2002) 82.
[14] G.T. Delgado, C.I.Z. Romero, S.A.M. Hernández, R.C. Pérez, O.Z. Angel, Sol. Energy Mater. Sol. Cells 93 (2009) 55.
[15] Y.X. Wang, X.Y. Li, G. Lu, X. Quan, G.H. Chen, J. Phys. Chem. C 112 (2008) 7332.
[16] Q. Wan, T.H. Wang, J.C. Zhao, Appl. Phys. Lett. 87 (2005) 083105.
[17] Y.H. Tong, J. Cheng, Y.L. Liu, G.G. Siu, Scripta Mater. 60 (2009) 1093.
[18] M. Dutta, D. Basak, Nanotechnology 20 (2009) 475602.
[19] F.M. Meng, X.P. Song, Z.Q. Sun, Vacuum 83 (2009) 1147.
[20] J. Xu, Y.G. Chang, Y.Y. Zhang, S.Y. Ma, Y. Qu, C.T. Xu, Appl. Surf. Sci. 255 (2008) 1996.
[21] M. Bizarro, Appl. Catal. B Environ. 97 (2010) 198.
[22] H.C. Yatmaz, A. Akyol, M. Bayramoglu, Ind. Eng. Chem. Res. 43 (2004) 6035.
[23] D. Raoufi, T. Raoufi, Appl. Surf. Sci. 255 (2009) 5812.
[24] G. Kenanakis, Z. Giannakoudakis, D. Vernardou, C. Savvakis, N. Katsarakis, Catal. Today 151 (2010) 34.
[25] L.Y. Zhang, L.W. Yin, C.X. Wang, N. Lun, Y.X. Qi, ACS Appl. Mater. Interfaces 2 (2010) 1769.
[26] J. Wang, P. Liu, X. Fu, Z. Li, W. Han, X. Wang, Langmuir 25 (2009) 1218.
[27] D. Behera, B.S. Acharya, J. Lumin. 128 (2008) 1577.
[28] X.D. Gao, X.M. Li, W.D. Yu, J. Solid State Chem. 177 (2004) 3830.
[29] S. Cho, J. Ma, Y. Kim, Y. Sun, G.K.L. Wong, J.B. Ketterson, Appl. Phys. Lett. 75 (1999) 2761.
[30] K. Vanheusden, W.L. Warren, C.H. Seager, et al, J. Appl. Phys. 79 (1996) 7983.
[31] X.L. Wu, G.G. Siu, C.L. Fu, et al, Appl. Phys. Lett. 78 (2001) 2285.